Misalignment-Tolerant Surface-Normal Low-Voltage Modulator for Optical Interconnects

Noah C. Helman, *Student Member, IEEE*, Jonathan E. Roth, David P. Bour, *Fellow, IEEE*, Hatice Altug, *Student Member, IEEE*, and David A. B. Miller, *Fellow, IEEE*

***Abstract*—We present a surface-normal modulator architecture for optical interconnects that offers misalignment tolerance as well as high contrast ratio over a wide wavelength range for a small drive voltage. A contrast ratio greater than 3 dB was achieved for only 0.8-V drive across a 16-nm wavelength range from 1498 to 1514 nm. The misalignment tolerance between this device, and the input optical beam was measured to be 30 μm.**

***Index Terms*—Fabry–Pérot resonators, optical interconnections, optical modulation, waveguides.**

I. Introduction

OPTICAL interconnects have been widely studied as a solution to the electrical interconnect bottleneck foreseen in computing systems [1]–[7]. The mature technology of Si CMOS electronics is well-established for high-speed information processing, while optical systems excel at information transmission. Future computing systems are likely to incorporate electronic components communicating along an optical channel that requires optoelectronic devices to convert signals from the electronic into the optical domain and *vice versa*.

Semiconductor optoelectronic modulators based on the quantum-confined Stark effect (QCSE) [8] are attractive transmitters for this application. Previous modulator designs can be grouped into two categories: surface-normal and waveguide geometries. Typical surface-normal devices suffer from a low interaction volume between the optical beam and the absorbing region of the device. Keeping the drive voltage down requires a thin absorption region, but this leads to a low contrast ratio. This tradeoff can be circumvented by placing the absorption region inside an optical resonator, as in asymmetric Fabry–Pérot modulator (AFPM) designs [9]–[11], at the expense of narrowing the wavelength range. Operation over a large range of wavelengths is necessary for optical systems that use wavelength-division multiplexing [7], [12] or uncooled laser sources. Thus, the challenge for surface-normal modulators is to achieve high contrast ratio, low drive voltage, and wide optical bandwidth in the same device. This is particularly difficult at 1500–nm wavelengths, where optical absorption in, e.g., InGaAs/InP structures is typically weaker overall than for the GaAs/AlGaAs structures that can be used for surface-normal operation at $\sim$ 850 nm. For these reasons, a great deal of research has focused on waveguide architectures for the longer wavelength modulators. However, coupling light from optical fibers into semiconductor waveguides is a challenge in practice. The high refractive index ($n \sim 3$–3.5) of the semiconductor waveguide yields a transverse optical mode much smaller than that of a fiber. This results in both large coupling loss and submicron alignment restrictions that significantly increase the cost of packaging waveguide modulators for commercial use.

This paper describes a novel modulator architecture called the quasi-waveguide angled-facet electroabsorption modulator (QWAFEM) that combines the best features of the surface-normal and waveguide geometries. Section II contains a general description of the device. Section III describes the techniques and results of our computer simulations using the transfer matrix method. Sections IV and V detail a demonstration of the QWAFEM in the InGaAsP/InP material system, including fabrication methods and experimental results.

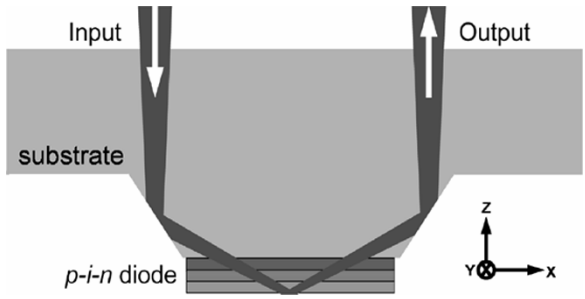

Fig. 1. Schematic of QWAFEM in cross section (not to scale).

II. The QWAFEM Concept

The QWAFEM is a *p-i-n* diode surrounded by two flat mirrors etched into the semiconductor substrate at equal angles, steeper than 45° with respect to the x axis, as shown in Fig. 1 [13]. The input laser beam passes through the transparent substrate and reflects off one angled mirror before entering the *p-i-n* diode at a large incident angle. The absorption of the light is modulated by the voltage applied across the diode, which typically contains multiple quantum wells (MQW). The beam then reflects off the semiconductor–air interface, passes back through the diode, reflects off the second angled mirror, and exits through the substrate.

Manuscript received July 15, 2004; revised January 2, 2005. This work was supported in part by the MARCO/DARPA Interconnect Focus Center through the Georgia Institute of Technology. The work of N. C. Helman and J. E. Roth was supported by the Gerhard Casper Stanford Graduate Fellowship and the National Science Foundation Fellowship, respectively.

N. C. Helman and H. Altug are with the Department of Applied Physics, Ginzton Laboratory, Stanford University, Stanford, CA 94305 (e-mail: nhelman@stanfordalumni.org).

J. E. Roth and D. A. B. Miller are with the Department of Electrical Engineering, Ginzton Laboratory, Stanford University, Stanford, CA 94305.

D. P. Bour is with the Communicatoins and Optics Research Laboratory, Agilent Laboaratories, 3500 Deer Creek Road, Palo Alto, CA 94304.

Digital Object Identifier 10.1109/JSTQE.2005.845613

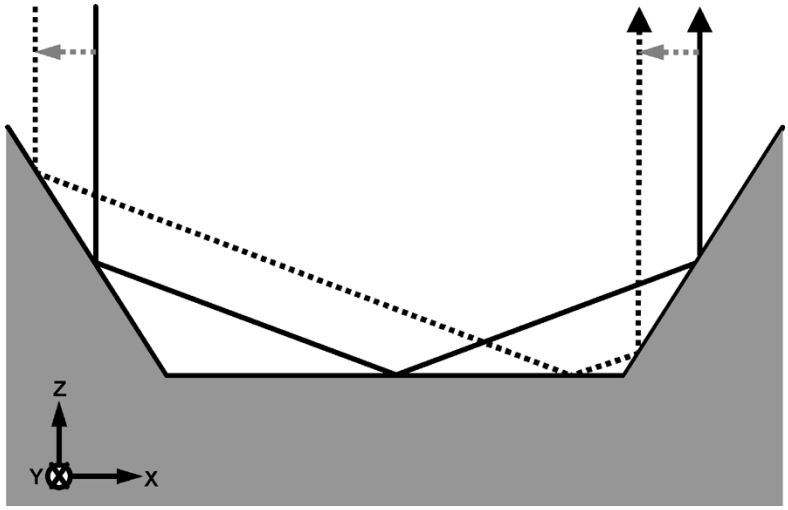

Fig. 2. Misalignment tolerance of three-bounce geometry. If the input beam is parallel to the z axis, its path can be translated in the x–y plane without changing the interaction with the modulator or the distance between the input and output beams.

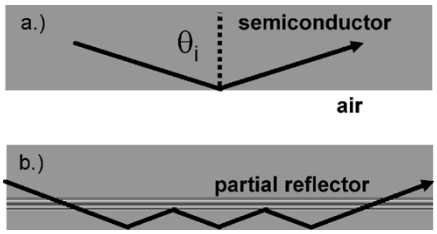

Fig. 3. (a) Reflection off a DBR with the angle of incidence θ_i indicated. (b) Adding another reflector increases the effective path length of a beam that is on resonance with the asymmetric Fabry–Pérot cavity.

This architecture has several advantages. Similar to the surface-normal geometry, the QWAFEM has its optical input and output in the z-direction enabling fabrication in two-dimensional (2-D) arrays. There is no mode matching constraint and the three-bounce geometry is inherently tolerant to misalignments of the device relative to the input beam, as illustrated in Fig. 2. Similar to the waveguide geometry, a high contrast ratio, wide optical bandwidth, and low-voltage drive operation can be achieved simultaneously.

The large angle of incidence θ_i of the laser beam onto the absorbing region has two significant effects. First, it increases the interaction volume of the light with the MQW by a factor of roughly $1/\cos\,\theta_i$. Second, it causes small differences in index of refraction to result in large Fresnel reflections. This enables the epitaxial growth of distributed Bragg reflectors (DBRs) with high reflectivity using only a small number of layer pairs. Incorporating a high-reflectivity DBR into the *n*-region results in a low-order AFPM structure (shown schematically in Fig. 3) that enhances the intensity of the optical wave inside the MQW region for a broad range of wavelengths.

III. Simulations

The optical design of the QWAFEM wafer was simulated using a semiempirical transfer matrix method [14]. In order to model the intrinsic MQW region, a wafer with a simple *p-i-n* structure was grown and the photocurrent was measured with respect to input wavelength and applied reverse bias. Using this data and the Kramers–Kronig relations, the absorption coefficient was calculated and converted into a complex index of refraction. The MQW region was subsequently modeled as a bulk material with a complex index of refraction that varied with wavelength in order to design a second wafer layer structure using the same quantum well design. This effective absorption coefficient versus wavelength is shown in Fig. 4(a) for various values of the electric field in the MQW generated by the applied reverse bias.

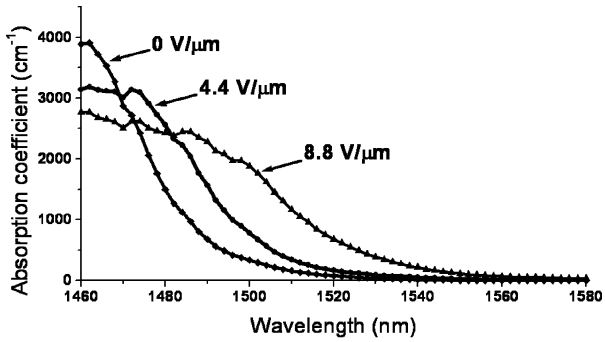

(a)

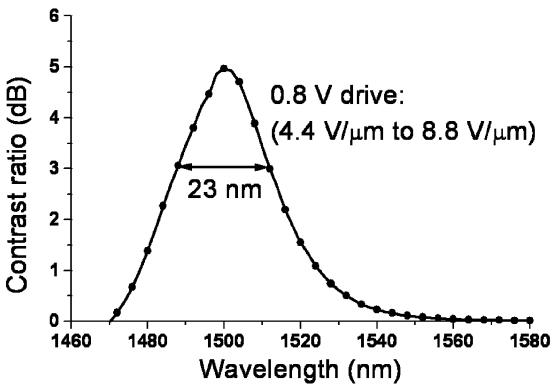

(b)

Fig. 4. (a) Experimental absorption coefficient versus wavelength for three values of the applied electric field in the MQW region: 0, 4.4, and 8.8 V/μm. (b) Contrast ratio simulation using the absorption coefficient shown in part a, illustrating a 23-nm wavelength range in which the contrast ratio exceeds 3 dB.

p-	InGaAs	25 nm
p-	InP	35 nm
p-	InGaAs	20 nm
p-	InP	93 nm
i-	MQW (8 QWs)	122 nm
n-	InP	233 nm
n-	InGaAsP (1.38 Q)	227 nm
n-	InP	278 nm
n-	InGaAsP (1.38 Q)	222 nm
n-	InP	354 nm
n-	InGaAsP (1.38 Q)	42 nm
SI	InP:Fe	substrate

Fig. 5. Numerically optimized wafer design.

Optimized structures using this method indicate the possibility of QWAFEM designs with peak contrast ratio $\sim$ 5 dB ($\sim$3.1 : 1), with an optical bandwidth (defined as contrast ratio $>$ 3 dB) over 23 nm, for a drive voltage of only 0.8 V [Fig. 4(b)]. The AFPM effect enabled the use of a thin intrinsic region (180 nm) such that the 0.8-V reverse bias swing alternated the applied electric field between 4.4 and 8.8 V/μm. Since the quantum wells are lattice matched and the absorption coefficient was derived from surface-normal photocurrent measurements, the complex refractive index of the MQW region is only valid for the TE polarization. (It is, of course, possible to design strained quantum wells that are polarization independent, but the optical properties of the device may still differ for the polarizations, due to the boundary conditions of Maxwell's equations at interfaces.) This simulation assumes TE polarization operation with a focused TEM_{00} Gaussian beam radius of 10 μm.

Simulations indicate the narrow angular resonance of such an AFPM structure. Though the input laser light resonates in the QWAFEM for a large range of wavelengths, it must impinge upon the *p-i-n* diode at an incident angle within a few degrees of the angle for which it was designed. Since a TEM_{00} Gaussian beam is composed of plane waves propagating at different angles, not all components of the beam will fall in the center of the resonance. An optical design with a stronger resonance (due to a higher reflectivity DBR) will have a narrower angular acceptance. Thus, an input with a larger focal beam waist has its energy distributed in a smaller angular range which couples more efficiently into the optical resonance of the QWAFEM design. Conversely, a tightly focused beam has a larger angular distribution and is modulated less efficiently.

IV. Wafer Design and Fabrication

To demonstrate this concept, the wafer structure simulated in Fig. 4 was grown via metal–organic chemical vapor deposition on semi-insulating (SI) Fe-doped InP substrates and QWAFEM devices were fabricated in the InGaAsP/InP material system. The *n*-region was a numerically optimized DBR stack of three pairs of alternating layers of InP and InGaAsP (lattice matched to InP and designed to have a bandgap wavelength of 1.38 μm) (Fig. 5). These layers were thicker than a surface-normal DBR by a factor of approximately $1/\cos\theta_t$ and the irregular thicknesses resulted from the optimization routine.

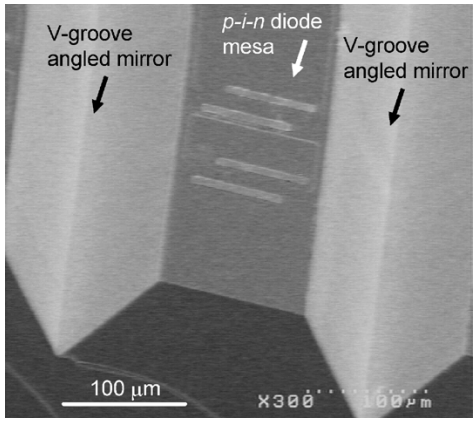

Fig. 6. Scanning electron micrograph of finished QWAFEMs.

The MQW region contained eight quantum wells lattice matched to InP, and the *p*-region was grown with thin layers of InGaAs/InP that can be selectively etched after fabrication to tune the resonant wavelength of the AFPM structure. Note that the dopants were offset from the intrinsic region on each side such that the total thickness of the undoped material was 180 nm. This wafer structure is relatively simple to grow due to the small number of lattice-matched quantum wells and the tolerance of the design to small changes in the layer thicknesses.

As shown in Figs. 1 and 6, QWAFEM devices are *p-i-n* diode mesas, surrounded on opposite sides by smooth V-grooves which act as the angled facets. The fabrication began with a simple *p-i-n* mesa structure. On two opposite sides of the mesas, a dry etch was used to remove the exposed epitaxial layers down into the middle of the 354-nm *n*-InP region.

The fabrication of the smooth angled facets in these areas is a multistep process. First, the remaining *n*-InP was removed with HBr. The 42 nm *n*-InGaAsP layer was used as an etch mask for the InP below. Rows on either side of the mesas were opened by etching the *n*-InGaAsP with $H_2SO_4 : H_2O_2 : H_2O$ (1 : 2 : 10). Next, V-grooves were etched into the InP substrate, similar to [15]. Ninety-micrometer-deep V-grooves were formed during a 24-min HBr wet etch (exposing the (111)A planes at an angle of 54.7° from the (100) plane). However, the surface roughness that resulted was too large ($\sim$ 250-nm rms) to use as a mirror. It was removed by a short wet etch in $HBr : K_2Cr_2O_7$ (1 : 1) at 65 °C (less than 1 s) [15]. White light interferometer measurements indicated the rms surface roughness was reduced to only 10–20 nm over 60–100-μm-wide sections of the angled mirror, and values as low as 1-5 nm have been observed previously. Finally, 2-D arrays of QWAFEMs were flip-chip bonded [16] with indium bumps onto gold wires on a glass substrate for testing.

V. Experimental Results

The reflectivity of the QWAFEMs was measured with respect to wavelength and voltage using a probe station equipped with a tunable laser source incident on the device in the TE polarization. The device under test was measured under various incident angles in order to compensate for a facet angle that deviated slightly (a few degrees) from the expected 54.7° due to undercutting during the facet smoothing process.

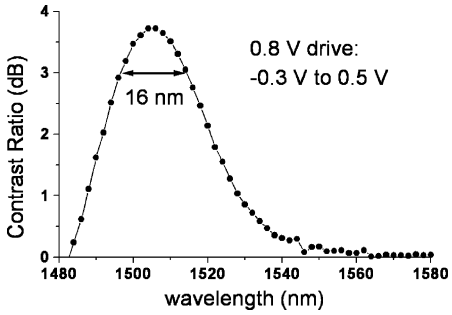

Fig. 7. Experimental contrast ratio versus wavelength for a QWAFEM for 0.8-V drive between −0.3-V and +0.5-V reverse bias.

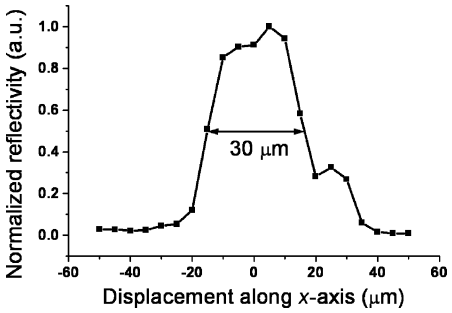

Fig. 8. Normalized reflectivity of a QWAFEM measured as a function of the lateral displacement of the device relative to the incoming optical beam to demonstrate the misalignment tolerance. The FWHM is 30 μm.

Fig. 7 shows the contrast ratio versus wavelength. A peak contrast ratio of 3.7 dB was achieved at 1506 nm with only 0.8 V of drive voltage. The contrast ratio was greater than 3 dB for a wavelength range of 16 nm from 1498 to 1514 nm and greater than 2 dB between 1492 and 1520 nm. The maximum change in absolute reflectivity was 10% at 1512 nm. The insertion loss at 1512 nm was measured to be −7.2 dB, which we believe is caused mostly by absorption in the *n*-InGaAsP layers and scattering from the angled mirrors (−6.7 dB) along with some quantum well (−0.3 dB) and substrate absorption (−0.2 dB).

The discrepancy between the simulated ($\sim$ 5 dB) and experimental (3.7 dB) contrast ratio was caused by inaccurate data regarding the refractive index of the *n*-InGaAsP (1.38 Q) layers during the design. A constant refractive index of 3.50 was used during simulations. More recently we had the opportunity to measure the refractive index experimentally with high accuracy and found that it varied significantly with wavelength between 3.45 and 3.42. By including this revised refractive index in the model, the simulated contrast ratio matches the experimental value around 3.7 dB.

In order to determine the misalignment tolerance, the QWAFEM was translated laterally relative to the input laser beam while measuring the output power. Fig. 8 shows the power as a function of lateral displacement in the x-direction. The full-width at half maximum (FWHM) of the reflected power for 0 V reverse bias is 30 μm. This value can be chosen somewhat arbitrarily by setting the size both of the angled mirrors lithographically and of the beam as it bounces off those mirrors.

VI. Conclusion

We presented a surface-normal electroabsorption modulator architecture that features a high contrast ratio over a wide wavelength range (16 nm) using a less than 0.8-V voltage drive along with a large misalignment tolerance of 30 μm. A peak contrast ratio of 3.7 dB was demonstrated for a 0.8-V drive. Simulations indicate that a peak contrast ratio of $\sim$ 5 dB is possible with a wavelength range of 23 nm over which the contrast ratio exceeds 3 dB. Further optimization of the quantum well design and the optical resonator structure may enable future devices to operate with higher contrast ratio at even lower voltage drive.

Acknowledgment

The authors wish to thank Dr. S. Bhalotra, N. Cao, T. Carver, Dr. H. V. Demir, O. Fidaner, and Dr. V. Sabnis for their assistance with various aspects of this project.

References

[1] D. A. B. Miller, "Physical reasons for optical interconnection," *Int. J. Optoelectron. (Special Issue on Smart Pixels)*, vol. 11, no. 3, pp. 155–168, 1997.

[2] ——, "Rationale and challenges for optical interconnects to electronic chips," *Proc. IEEE*, vol. 88, no. 6, pp. 728–749, Jun. 2000.

[3] J. W. Goodman, F. J. Leonberger, S. Y. Kung, and R. A. Athale, "Optical interconnections for VLSI chips," *Proc. IEEE*, vol. 72, pp. 850–866, Jul. 1984.

[4] X. Zheng, P. J. Marchand, D. Huang, and S. Esener, "Free-space parallel multichip interconnection system," *Appl. Opt.*, vol. 39, no. 20, pp. 3516–3524, Jul. 2000.

[5] V. Baukens, I. Veretennicoff, and H. Thienpont, "Free-space optical interconnection modules for two-dimensional photonic very large scale integration circuitry based on microlenses and gradient-refractive-index lenses," *Opt. Eng.*, vol. 40, no. 11, pp. 2431–2441, Nov. 2001.

[6] M. P. Christensen, P. Milojkovic, M. J. McFadden, and M. W. Haney, "Multiscale optical design for global chip-to-chip optical interconnections and misalignment tolerant packaging," *IEEE J. Sel. Topics Quantum Electron.*, vol. 9, no. 2, pp. 548–556, Mar./Apr. 2003.

[7] B. E. Nelson, G. A. Keeler, D. Agarwal, N. C. Helman, and D. A. B. Miller, "Wavelength division multiplexed optical interconnect using short pulses," *IEEE J. Select. Topics in Quantum Electron.*, vol. 9, no. 2, pp. 486–491, Mar./Apr. 2003.

[8] D. A. B. Miller, D. S. Chemla, T. C. Damen, A. C. Gossard, W. Wiegmann, T. H. Wood, and C. A. Burrus, "Electric-field dependence of optical absorption near the bandgap of quantum well structures," *Phys. Rev. B*, vol. 32, pp. 1043–1060, 1985.

[9] S. J. B. Yoo, M. A. Koza, R. Bhat, and C. Caneau, "1.5 mm asymmetric Fabry–Perot modulators with two distinct modulation and chirp characteristics," *Appl. Phys. Lett.*, vol. 72, no. 25, pp. 3246–3248, Jun. 1998.

[10] C. C. Barron, C. J. Mahon, B. J. Thibeault, and L. A. Coldren, "Design, fabrication, and characterization of high-speed asymmetric Fabry–Perot modulators for optical interconnect applications," *Opt. Quantum Electron.*, vol. 25, no. 12, pp. 5885–5895, Dec. 1993.

[11] K. K. Law, M. Whitehead, J. L. Merz, and L. A. Coldren, "Simultaneous achievement of low insertion loss, high contrast and low operating voltage in asymmetric Fabry–Perot reflection modulator," *Electron. Lett.*, vol. 27, no. 20, pp. 1863–1865, Sep. 1991.

[12] F. Zhao, Y. Zhang, J. Z. Zou, Z. Shi, B. Bihari, E. Frietman, X. G. Deng, J. Qiao, Z. Shi, and R. T. Chen, "Wavelength division multiplexers/demultiplexers for optical interconnects in massively parallel processing," *Opt. Eng.*, vol. 42, no. 1, pp. 273–280, Jan. 2003.

[13] N. C. Helman, J. E. Roth, D. P. Bour, and D. A. B. Miller, "Misalignment-tolerant low-voltage surface-normal optoelectronic modulator for optical interconnects at 1.5 μm," presented at the Conf. Lasers and Electrooptics, San Francisco, CA, 2004.

[14] H. A. MacLeod, *Thin Film Optical Filters*. Philadelphia, PA: IoP, 2001.

[15] P. Bonsch, D. Wullner, T. Schrimpf, A. Schlachetzki, and R. Lacmann, "Ultrasmooth V-grooves in InP by two-step wet chemical etching," *J. Electrochem. Soc.*, vol. 145, no. 4, pp. 1273–1276, Apr. 1998.

[16] K. W. Goossen, J. A. Walker, L. A. Dasaro, S. P. Hui, B. Tseng, R. Leibenguth, D. Kossives, D. D. Bacon, D. Dahringer, L. M. F. Chirovsky, A. L. Lentine, and D. A. B. Miller, "GaAs MQW modulators integrated with silicon CMOS," *IEEE Photon. Technol. Lett.*, vol. 7, no. 4, pp. 360–362, Apr. 1995.

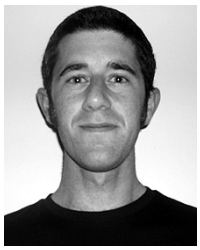

Noah C. Helman (S'02) received the A.B. degree in physics from Harvard University, Cambridge, MA, in 1998 and the M.S. degree in applied physics from Stanford University, Stanford, CA, in 2002. He is currently working toward the Ph.D. degree in applied physics under Prof. D. A. B. Miller at Stanford University, and will receive the degree in June 2005. His dissertation focuses on optoelectronic modulators for optical interconnects.

Jonathan E. Roth received the B.S. degree in biomedical engineering from Case Western Reserve University, Cleveland, OH, in 2000. He is currently working toward the Ph.D. degree in electrical engineering at Stanford University, Stanford, CA, under Prof. D. A. B. Miller.

From 2000 to 2001, he was involved in research as a Fulbright grantee at Lund Institute of Technology, Lund, Sweden, studying optical properties of tissue and photodynamic therapy. His current research focuses on optoelectronic modulators.

David P. Bour (S'84–M'87–SM'97–F'00) received the B.S. degree in physics from the Massachusetts Institute of Technology, Cambridge, in 1983, and the Ph.D. degree in electrical engineering from Cornell University, Ithaca, NY, in 1987.

From 1987 to 1991, he was a Member of Technical Staff at the Sarnoff Corporation. From 1991 to 1999, he was a Principal Scientist in the Electronic Materials Laboratory of the Xerox Palo Alto Research Center, fabricating nitride blue laser diodes and phosphide red laser diodes for laser printing. He is currently an Agilent Fellow in the Photonics and Electronics Research Laboratory at Agilent Laboratories, Palo Alto, CA, where he is working on the epitaxial growth of semiconductor lasers by metal–organic chemical vapor deposition.

Hatice Altug (S'02) received the B.S. degree in physics from Bilkent University, Ankara, Turkey, in 2000. She is currently working toward the Ph.D. degree in applied physics at Stanford University, Stanford, CA.

Her research interests include the design and fabrication of photonic crystal-based optical devices.

David A. B. Miller (M'84–SM'89–F'95) received the B.Sc. degree from St. Andrews University in 1976 and the Ph.D. degree from Heriot-Watt University in 1979.

He was with Bell Laboratories from 1981 to 1996 as a department head from 1987, latterly of the Advanced Photonics Research Department. He is currently the W. M. Keck Professor of Electrical Engineering at Stanford University, Stanford, CA, and the Director of the Ginzton and Solid State and Photonics Laboratories, Stanford, CA. He has published more than 200 scientific papers and holds over 55 patents. His research interests include quantum-well optoelectronic and nanophotonic physics and devices, and fundamental and applications of optics in information, sensing, switching, and processing.

Dr. Miller has served as a Board Member for both the Optical Society of America (OSA) and the IEEE Lasers and Electro-Optics Society (LEOS), and in various other society and conference committees. He was President of the IEEE Lasers and Electro-Optics Society in 1995. He was awarded the Adolph Lomb Medal and the R. W. Wood Prize from the OSA, the International Prize in Optics from the International Commission for Optics, and the IEEE Third Millennium Medal. He is a Fellow of the Royal Societies of London and Edinburgh, the OSA, and the American Physical Society (APS) and holds honorary degree from the Vrije Universiteit Brussel and Heriot-Watt University.